Vacuum 204 (2022) 111339

Contents lists available at ScienceDirect

Vacuum

journal homepage: www.elsevier.com/locate/vacuum

# Effect of the magnetic field on the operation of ionisation gauges

Ricardo A.S. Silva *, Nenad Bundaleski, Orlando M.N.D. Teodoro

CEFITEC, Department of Physics, Nova School of Science&Technology, Nova University Lisbon, 2829-515, Caparica, Portugal

ARTICLE INFO

*Keywords:*
Ionisation vacuum gauges
Magnetic field
Simulation
SIMION
Sensitivity

ABSTRACT

Hot cathode ionisation gauges are the only reliable pressure measurement devices suitable for both high and ultra-high vacuum measurement. These devices are characterized by low accuracy that is hardly better than 20%. The sources of loss of accuracy are documented in the literature although their quantification and details are not fully understood. In the present work, simulations of Bayard-Alpert and extractor gauges were performed under the influence of uniform magnetic fields up to 30 Gs. Results are in qualitative agreement with measurements taken previously with the Bayard-Alpert gauge. Both gauges are sensitive to low intensity magnetic fields which may be present in vacuum chambers. However, the extractor gauge proved to be more stable in the presence of a magnetic field due to its ring-shaped cathode.

## 1. Introduction

Ionisation vacuum gauges are indispensable pressure measuring devices at high vacuum and lower pressures, both in industry and research [1]. In spite of its significance, accurate pressure measurement in this range remains to be a challenge. Common ionisation gauges, such as Bayard-Alpert (BA) or Penning type, have typical uncertainties for nitrogen up to 20% [2–7]. The situation is clearly worse for other gases [3,7,8], compromising pressure measurements with the accuracy required in different applications beyond metrology.

Hot cathode ionisation gauges lack robustness of their construction (e.g., anode and particularly ion collector of BA gauges are both made of very thin wires), causing changes of its geometry during the operation and transportation. The latter appears to be one of the major reasons for the uncertainties in hot cathode ionisation gauges, due to their influence on the mean electron path length inside the ionisation volume [7]. In addition, measurements are affected by different particle-electrode interactions, such as X-ray emission, electron stimulated desorption and electron backscattering from the anode, as well as ion induced secondary electron emission from the ion electrode [7,9]. The majority of these phenomena contribute to the low pressure limit of ionisation gauges, thus affecting the measurement accuracy at low pressures. Besides, any change of electrodes' surface will decrease the measurement repeatability and reproducibility.

A few ionisation gauges were developed with an improved design to reduce the measurement limitations. One is the extractor gauge, in which the ion collector is hidden from the anode, reducing the fraction of anode area with which the collector has direct line of sight. Such a construction strongly reduces the contribution of X-rays to the ion collector current [10,11]. The design of this gauge also reduces considerably the collection of desorbed ions released on the anode due to their higher energy in respect to gas phase ions [11,12]. Although with reduced sensitivity, these features extend its application towards lower pressures well in the UHV and XHV ranges (ultra-high and extreme vacuum). Low influence of secondary particles on its operation also contributes to the long-term stability of 2.5% [3], being a considerable improvement with respect to the BA gauges type. Another solution is the Stabil-Ion gauge, which is a BA-type gauge with more robust construction providing well-defined and stable geometry [2]. The latter is characterised with significantly increased accuracy with respect to common BA gauges (~4%), although showing a long-term stability somewhat lower than that of the extractor gauge [3].

Recently, a novel ionisation gauge suitable as a reference standard in the $10^{-4}$-$10^{-8}$ mbar range was developed in the frame of the European project 16NRM05 'Ion gauge' (EMPIR programme) [13]. Apart from a very good repeatability (<0.05%) and reproducibility (<1%) for different gases, even after cathode replacement, this gauge even provides predictable sensitivity within 1.5% [14]. These outstanding results are achieved by a design in which an electron beam makes a single pass throughout the ionisation volume, ending inside of a Faraday cup without a direct line of sight with the ion collector. Authors found that weak magnetic fields can have strong influence on its operation (in some directions, magnetic field of only 2 Gs disables the gauge), which is why Mu-metal shielding is recommended [13].

* Corresponding author.
*E-mail address:* ras.silva@campus.fct.unl.pt (R.A.S. Silva).

https://doi.org/10.1016/j.vacuum.2022.111339
Received 4 May 2022; Received in revised form 11 July 2022; Accepted 12 July 2022
Available online 16 July 2022

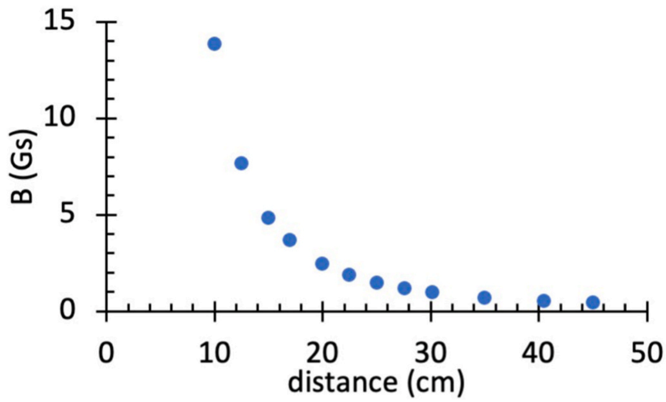


**Fig. 1.** Measured magnetic field distribution along the axis of the Penning gauge IKR 251 Pfeiffer. The magnetic field is directed along the Penning gauge. Distance of 0 cm corresponds to the position of the connecting flange.

Conventional hot cathode ionisation gauges can hardly operate in magnetic fields of the order of hundreds of Gs, which can even affect the filament shape [15]. Similar problems in the same range of the magnetic field were observed in quadrupole mass spectrometers [16]. These issues motivated a development of the ASDEX gauge suitable for fusion reactors, which are characterized by strong magnetic fields [17]. Having this in mind, one may ask: what would be the influence of a small magnetic field of a few tens of Gauss on the operation of conventional ionisation gauges? Since magnetic fields of several Gs already affect electron trajectories with a few hundred eV of energy, this influence is inevitable in common ionisation gauges.

Magnetic fields of some tens of Gs are commonly present in vacuum systems, e.g., in the vicinity of ion pumps or Penning gauges. As an example, the measured distribution of magnetic field along the symmetry axis of the Penning gauge (model IKR 251, Pfeiffer) is presented in Fig. 1. Even at a distance of 20 cm from a Penning gauge, one can expect a significant change on the electron trajectories [13]. Consequently, knowing that gauges with accuracy of about 5% are commercially available, the influence of magnetic fields on their operation can hardly be ignored. To the best of our knowledge, there is only one publication with systematic studies of the influence of magnetic field in this range on the operation of ionisation gauges [18]. The aim of this study is to fill this gap to some extent.

In the present work we discuss the influence of uniform magnetic fields, up to 30 Gs, on the operation of BA and extractor ionisation gauges. For that purpose, a previously developed simulation tool for studying ionisation gauges, based on the well-known software for charged particle optics, SIMION ver. 8.1, was used [19]. In this previous work, authors have shown a very good agreement with other simulation tool and corresponding experimental measurements [19,20]. In addition, the same tool was used to simulate deflection of the primary electron beam by the magnetic field in the novel ionisation gauge, allowing to determine its geometric profile. The simulated beam profile agrees very well with the experimental one, demonstrating capability of the simulation tool to successfully model the effect of a uniform magnetic field [21].

In 1981, H. C. Hseuh carried out an exhaustive test of a BA operation in the presence of weak magnetic fields [16]. A modified Granville Phillips series 274 was tested at magnetic fields between 5 and 60 Gs for different directions. The ion current was measured as a function of the magnitude of B and magnetic fields were generated by two permanent magnets. The distance between magnets was varied between 10 and 25 cm to change the magnitude of B in the volume of BA. Due to the method used, the homogeneity of B varies up to ±30% within the grid volume.

In the present work, simulation results are compared with experimental measurements obtained by H. C. Hseuh for the case of BA gauge. A similar work for the extractor gauge was not found.

Although the comparison is mainly of a qualitative nature, due to different geometries of the two BA gauges, quantitative agreement was also achieved to a large extent. The same approach provides a novel insight into the operation of an extractor gauge, suggesting a smaller influence of magnetic fields <30 Gs on the sensitivity as compared to the BA gauges.

## 2. Methods

The influence of magnetic field on the operation of ionisation gauges was studied. SIMION was used to study the influence of a weak magnetic field (<30 Gs) on two different ionisation gauges - the BA gauge (manufactured at CERN, see Ref. [20]) and the extractor gauge (following the geometry of the Inficon manufacturer). The geometry and

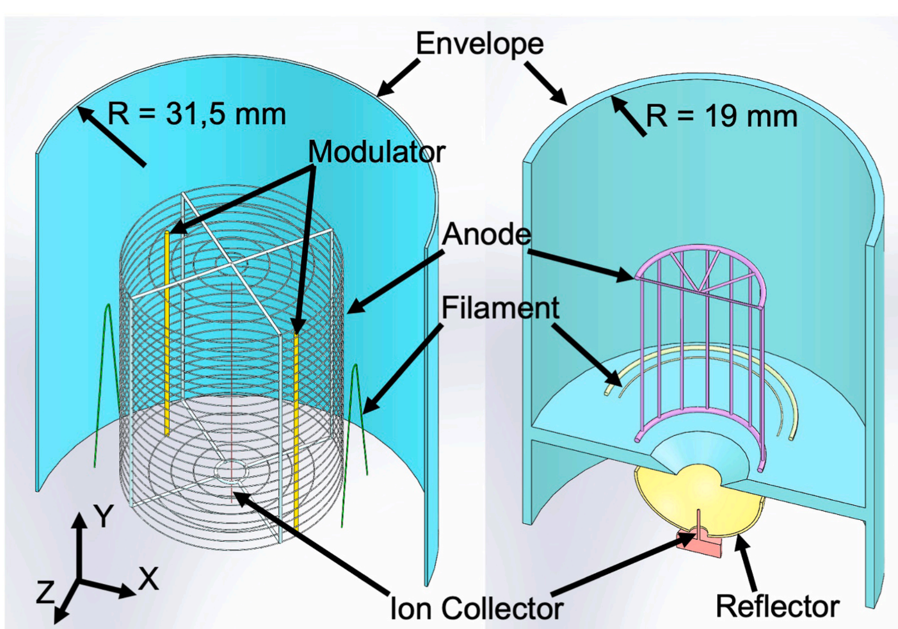


**Fig. 2.** Geometry of simulated ionisation gauges: Bayard-Alpert (left); extractor (right).

**Table 1**
Dimensions (mm) and potentials (V) of the gauges' electrodes.

| Gauge | Electrode | Dimension | Wire Diameter | Potential |
|---|---|---|---|---|
| BA | Anode grid | Ø 35 × 45 | Ø 0,13 | 150 |
| | Filament | Height 30 | Ø 0,18 | 50 |
| | Modulator | Length 42 | Ø 0,7 | 150 |
| | Collector | Length 42 | Ø 0,05 | 0 |
| | Envelope | Ø 63 | – | 0 |
| Extractor | Anode grid | Ø 14 × 24,70 | Ø 0,3 | 220 |
| | Filament | Ø 18 | Ø 0,15 | 100 |
| | Filament support | Ø 21 | Ø 0,5 | 100 |
| | Collector | 4,5 | Ø 0,3 | 0 |
| | Reflector | R7 | – | 205 |
| | Envelope | Ø 38 | – | 0 |

potentials of these gauges are illustrated in Fig. 2.

The BA gauge consists of 2 filaments, an anode made of thin wires forming a cylindrical shape, two modulators to subtract the influence of X-rays and an ion collector in the form of a filament of 50 μm in diameter. In the simulation the gauge was mounted inside of a metallic tube with a diameter of 63 mm (envelope) at a potential of 0 V.

The extractor gauge has a ring-shaped filament that surrounds the anode. In this sensor, the ion collector is hidden from the anode in the center of a hemisphere, which serves as a reflector to focus ions on the collector. The gauge was assumed to be mounted inside of a grounded metallic tube with 38 mm in diameter. Dimensions and potentials of the gauges' electrodes are summarized in Table 1.

The simulation approach is similar to that in Ref. [19]. Briefly, the ion current in a hot cathode ionisation gauge will be given by the expression

$$I_i = I_e \cdot S \cdot p \tag{1}$$

where $I_e$ represents the electron emission current, $p$ the gas pressure and $S$ a constant commonly named sensitivity [7]. This quantity characterizes the gauge in terms of its efficiency in ionizing and collecting the created ions. The approximate value of this constant is given by

$$S = \frac{\langle L \rangle \cdot \sigma}{k_B \cdot T} \cdot P_c \tag{2}$$

where $\langle L \rangle$ represents the mean value of the electron path length $L$, $\sigma$ the electron impact ionisation cross section, $T$ the gas temperature and $P_c$ the probability of collection of an ion once ionisation occurs [7]. The above expression is based on the assumption that the electron energy is constant along its trajectory.

In a more realistic approach, the electron energy is changing along its trajectory, which brings us to a more general expression for the ionisation gauge sensitivity:

$$S = \frac{\left\langle \int_0^L \sigma(E) dl \right\rangle}{k_B \cdot T} \cdot P_c \tag{3}$$

in which the variation of the energy dependent cross section is considered. This expression can be further simplified assuming $P_c$ approaching 1 inside the anode volume, and 0 in the rest of the volume. This assumption is justified for the BA gauge [20] and extractor gauge [22] gauges. This condition is maintained even in the presence of a magnetic field <60 Gs as used in the present work, since ions are much slower than electrons. Therefore, expression (3) can be rewritten as follows

$$S = \frac{\int_{inside} \sigma(E) dl}{k_B \cdot T} \tag{4}$$

where ionisation cross section is integrated only along the path inside the anode volume.

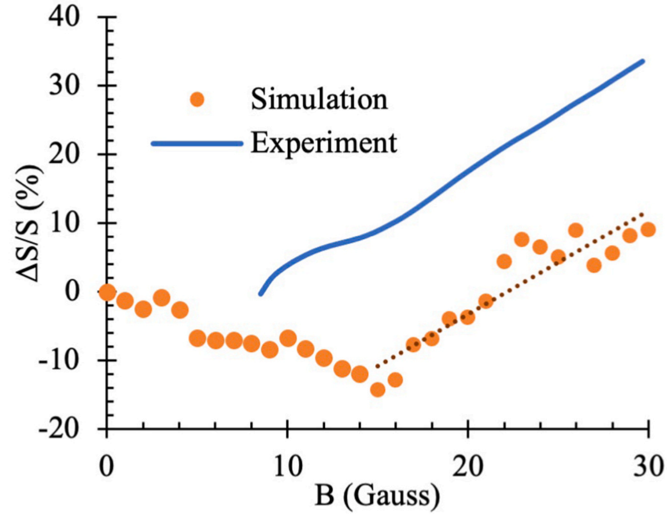


**Fig. 3.** Relative change of BA sensitivity as a function of magnetic field intensity along the x-axis: simulation – dots; empirical – line [18].

In the presence of a magnetic field, electrons trajectories will change, having direct consequence on the gauge sensitivity due to different path lengths within the anode volume. Relative change of gauge sensitivity due to changed electron trajectories (caused by different reasons including the magnetic field) can be expressed as

$$\frac{\Delta S}{S} = \frac{\Delta < \int_{inside} \sigma(E) \mathrm{d}l >}{< \int_{inside} \sigma(E) \mathrm{d}l >} \tag{5}$$

To model gauges in SIMION, their geometry was defined in CAD software and imported into SIMION using the SL Tools utility, converting each electrode into a PA file (potential array file). Resolution used for the conversion was 0.05 and 0.1 mm/gu (gu = grid unit) for BA and extractor gauge, respectively. These resolutions were selected to not significantly compromise simulation results due to discretisation and, on the other hand, not to make the simulation excessively heavy. To calculate the potential distribution with SIMION, by solving the Laplace equation, a convergence limit of $10^{-6}$ V was defined. A smaller convergence limit did not influence the simulation results.

In simulations we follow the relative change of sensitivity, calculated according to expression (5), as a function of the external magnetic field. The magnetic field in the simulations was uniform and oriented along the x, y and z axes (cf. Fig. 2). The field intensities were changed in the range from 0 to 30 Gs, with a step of 1 Gs. In each simulation, 5000 electron trajectories were calculated. Electrons were uniformly emitted from the filament surface into a solid angle of $2\pi$ with a constant initial energy of 0.1 eV. Preliminary simulations revealed that the influence of the initial conditions is negligible doe to the strong field accelerating electrons towards the ionisation volume. The energy dependence of the cross section for electron impact ionisation of N2 was taken from the NIST database [23], the latter being based on the BEB method [24].

## 3. Results and discussion

### *3.1. BA gauge*

In the case of the BA gauge, magnetic field was applied along the 3 axes of the Cartesian system presented in Fig. 2. In Fig. 3 shows the variation of the sensitivity as function of a field along the x-axis (i.e., along the direction of electron acceleration), revealing a steady decrease down to 14% for 15 Gs followed by a rise up to 9% at 30 Gs. The corresponding results of an experiment, performed on other BA gauge in the range 10–30 Gs (solid line), show the same general tendency in the range of 15–30 Gs (dotted linear line) [18]. It should be emphasized that

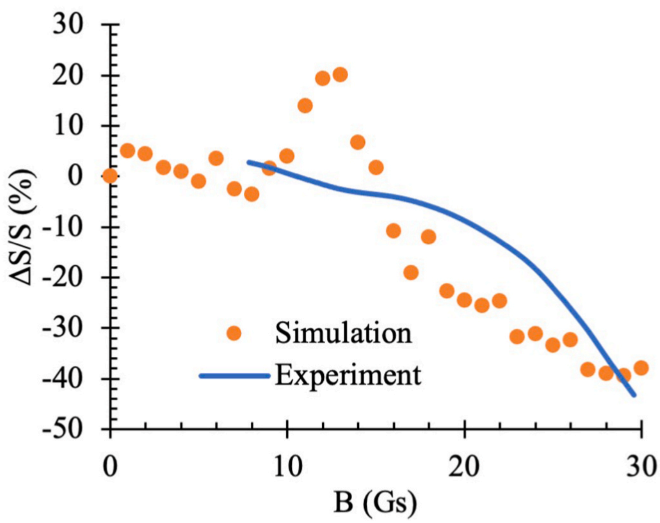


**Fig. 4.** Relative change of BA sensitivity as a function of magnetic field intensity along the y-axis: simulation – dots; the continuous line is plotted with data taken from Ref. [18].

good agreement cannot be expected due to different BA geometries and the inhomogeneity of the magnetic fields and directions in the measurements. Nevertheless, both results show that relative sensitivity change up to 20% can be expected in this range of magnetic field.

Simulations do not provide clear correlation between changes of trajectories and sensitivity with magnetic fields. The field is aligned with the electron velocity in the first few millimetres, forcing the electrons to have a helical path along the x-axis. However, once they pass through the anode grid, their paths diverge from the x-axis, creating a swarm of electrons to which we cannot ascribe representative paths.

When applying the field along the gauge axis (y-axis in Fig. 2), the sensitivity change is more pronounced, as shown in Fig. 4. Both, the simulation and the experiment, demonstrate a decrease in sensitivity down to approximately 40% for 30 Gs. However, there is a pronounced maximum of about +20% between 10 and 15 Gs.

Fig. 5a) shows the effect of a magnetic field on a typical electron trajectory. In the absence of field, the projection of the electron trajectories on the xz plane have a typical triangular shape as a result of the field distribution produced by the anode, the ion collector and the outer envelope (at 0 V) [19]. When the magnetic field is applied, it always bends the trajectories towards the anode, not allowing electrons to penetrate deeply into the useful ionisation volume. More importantly, such trajectories increase their frequency of passage through the anode and consequently the probability of collision with this electrode. This causes a decrease of the mean electron path length and, therefore, of sensitivity. The local sensitivity maximum at 13 Gs is related to the construction details of the anode grid. The latter consists of two relatively thick rectangular frames to which the Ø 0.05 wire is spot welded (cf. Fig. 2). It appears that when the field is close to 13 Gs the electron beam is guided in such way that it systematically avoids the vertical pillars of the rectangular frames. This results in a significant increase in the mean path length, as it can be seen in Fig. 5b). Despite the smaller length of each passage inside the anode, the overall sensitivity is considerably increased since the number of passages is highly increased. This local sensitivity maximum seems specific to this version of the Bayard-Alpert gauge and should not be generally expected.

Applying magnetic field along the z-axis also reduces the gauge sensitivity, which is confirmed by the previous experiments [18]. With a field intensity of 30 Gs the sensitivity is reduced by about 35%, as illustrated in Fig. 6. Although the final result is the same, the simulation shows an inverted behaviour between 8 and 18 Gs when compared with the experiment of H. C. Hseuh. Trajectories plotted in Fig. 7 provide the reason for the observed decrease in sensitivity. Similarly to the previous direction, the electrons have initial velocities perpendicular to the magnetic field. This causes intense bending of the trajectories leading to an increase in the frequency of passage through the anode. Again, the trajectories in the ionisation volume of interest are shortened due to the increased probability of anode impact, yielding in the decreased sensitivity.

Simulation results above show a generally good quantitative and qualitative agreement with experimental measurements. Observed differences are most probably caused by geometry and construction details, as it was illustrated in the case of the intense sensitivity maximum at 13 Gs along y-axis. These results confirm that the used simulation model is suitable for predicting the influence of magnetic fields on the operation of ionisation gauges. It also provides insight on the reason for the changes in sensitivity and adds what can be expected for B < 6 Gs.

### *3.2. Extractor gauge*

In the case of the extractor gauge, the simulations were carried out with magnetic fields only along the radius (x axis) and along the gauge axis (y axis) due to its cylindrical symmetry. This symmetry plays an important role concerning the magnetic field influence. In extractor gauge, the electrons' initial velocity is radial and it has different directions along the cathode, contrary to what happens in BA, where all electrons have initial velocities with similar directions.

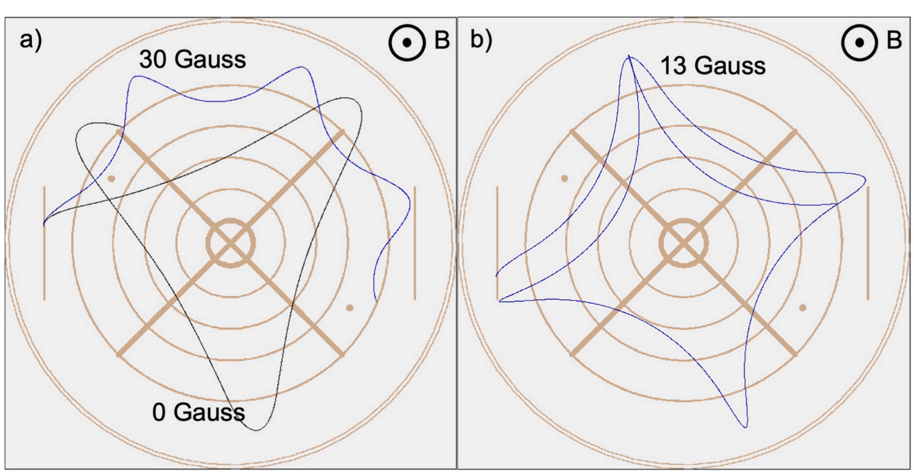


**Fig. 5.** Simulation of the electron trajectories inside the BA gauge: a) two trajectories of the same electron, with 30 Gs along y-axis and without magnetic field, blue and black lines, respectively; b) trajectory of one electron with magnetic field of 13 Gs along the y-axis.

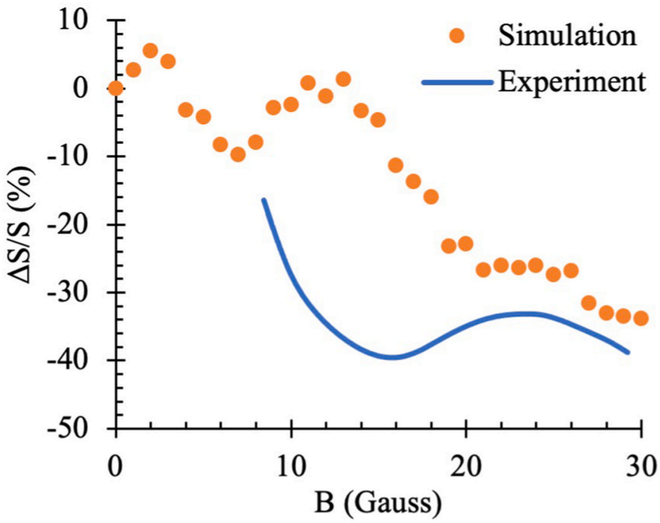


**Fig. 6.** Relative change of BA sensitivity as a function of magnetic field intensity along the z-axis: simulation – dots; the continuous line is plotted with data taken from Ref. [18].

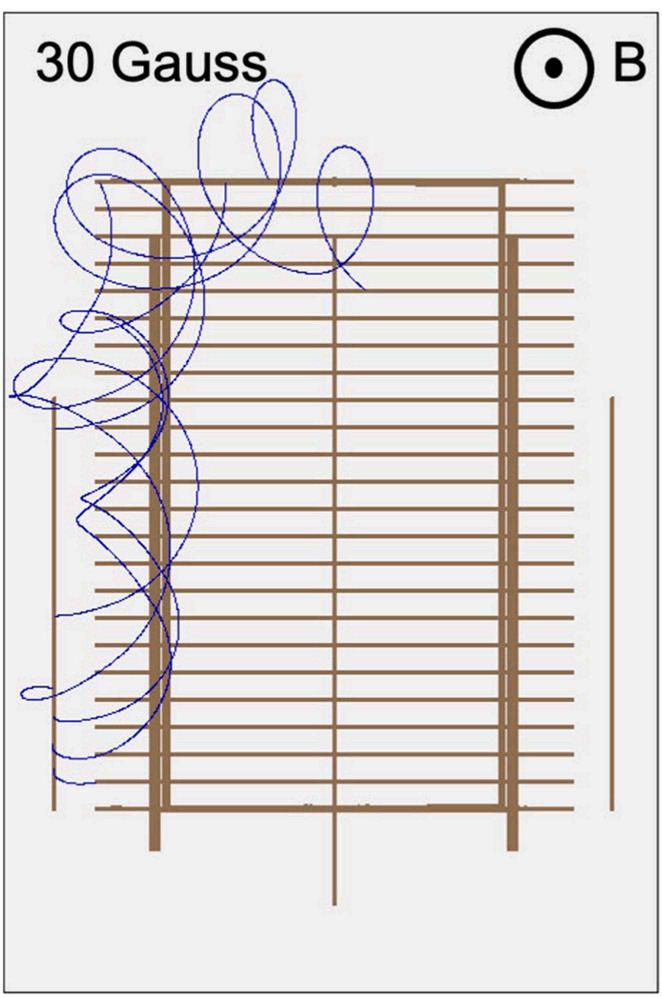


**Fig. 7.** Electron trajectories in the presence of a 30 Gs magnetic field intensity along the z-axis.

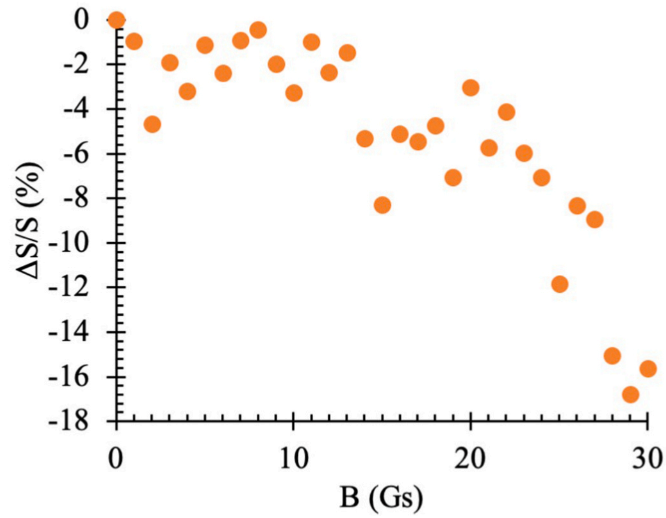


**Fig. 8.** Relative change of extractor gauge sensitivity as a function of magnetic field intensity along the x-axis.

Fig. 8 shows that, when the magnetic field is applied along the radial direction, the sensitivity tends to decrease, but the actual relative drop is significantly smaller than in the case of the BA gauge for any field direction. Indeed, this drop is below 10% up to 25 Gs, reaching only 17% for 30 Gs.

Fig. 9 presents the beginning of many electron trajectories starting in different position on the filament (before their end i.e., interrupted trajectories) in order to make the general trends more visible. Trajectories show symmetry in their modification by the radial magnetic field - Lorentz force acting on electrons emitted from opposite sides of the ring-shape filament will have the same intensity but opposite sign. Similar to what happened in the BA gauge simulation, with the magnetic field along the z-axis (normal to the initial electron velocity), the presence of a magnetic field increases the probability of impact on the anode, thus contributing to the reduced electron mean path within the ionisation volume. That effect should be taking place in the extractor gauge for electrons emitted from most of the filament when the initial trajectories are not collinear with the magnetic field. For those electrons that are emitted collinearly with the magnetic field, the effect on the path length inside the anode should be smaller. Since part of the emitted current is always much less affected by the magnetic field, the variation in sensitivity is less pronounced in the presence of a radial magnetic field.

As depicted in Fig. 10 if the magnetic field is applied along the gauge axis the sensitivity decreases for about 15% at 28 Gs, reaching about 26% at 30 Gs. The reason is clear from the interrupted trajectories presented in Fig. 11. The Lorentz force acts on all electrons in the same way, bending their trajectories in the plane. In the top view, we notice that most trajectories are bent counterclockwise while in the absence of field both bending directions are seen. As in the case of the BA gauge, the magnetic field increases the frequency of passage through the anode mesh, decreasing the length of its trajectory.

These simulations shows that sensitivity of the extractor gauge is less affected by the magnetic field than a BA gauge, whichever is its direction. Possibly, the main reason for the greater stability of the extractor gauge is related with the cathode geometry. The ring-shaped cathode leads to a lower influence of a magnetic field on the electron trajectories, thus reducing its effect on the sensitivity.

The trend that more uniform trajectories, with less divergence in the velocity directions, impose higher impact of magnetic field on gauge operation is rather general. A very good example is the recently proposed ISO gauge with primary electrons in the form of a beam [13], in contrast to the gauges considered in this study that operate with swarms of primary electrons. Despite the superior accuracy of the ISO gauge, it

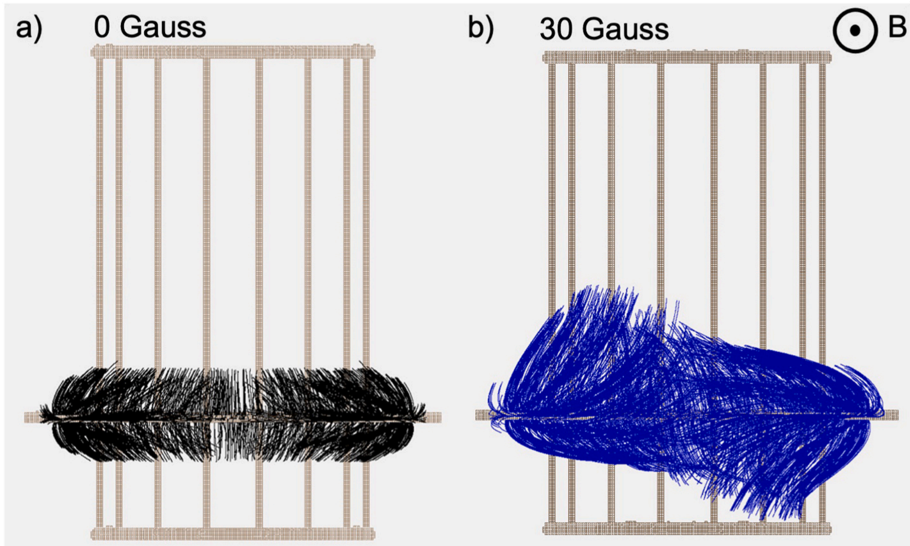


**Fig. 9.** Interrupted simulation of the electron trajectories inside the extractor gauge: a) without magnetic field; b) with magnetic field of 30 Gs along the x-axis.

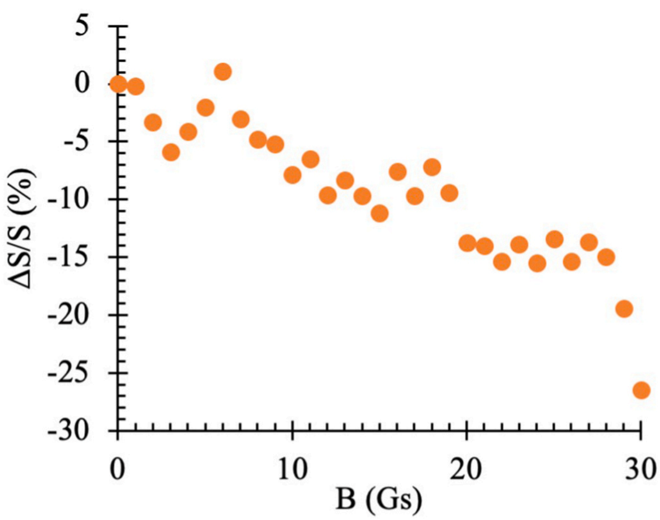


**Fig. 10.** Relative change of extractor gauge sensitivity as a function of magnetic field intensity along the y-axis.

cannot even operate under a magnetic field of only 2 Gs perpendicular to the gauge axis without proper shielding. The same field changes the sensitivity of a BA or extractor gauge for about 5% or less.

## 4. Conclusion

In this study, numerical simulations were carried out in order to investigate the influence of weak magnetic fields on the operation of two frequently used hot cathode ionisation gauges: BA gauge and extractor gauge. Results indicate that fields up to 30 Gs, which may be present in vacuum chambers, can introduce measurement errors of 5–30%. This should be considered whenever magnetic circuits are nearby and when accurate pressure measurements are required.

Simulation of a BA gauge shows similar tendencies to those measured on a BA gauge, with somewhat different geometry, performed by Ref. [18]. Sensitivity change in both gauges is comparable, while the details of the sensitivity vs. magnetic field dependence are determined by the details of each geometry.

In the case of the extractor gauge, experimental data were not available to compare with. However, simulation results clearly suggest higher stability of this gauge than a BA. A main reason appears to be related with the increased radial symmetry (which includes also the cathode) which cancels the sensitivity change due to modified electron

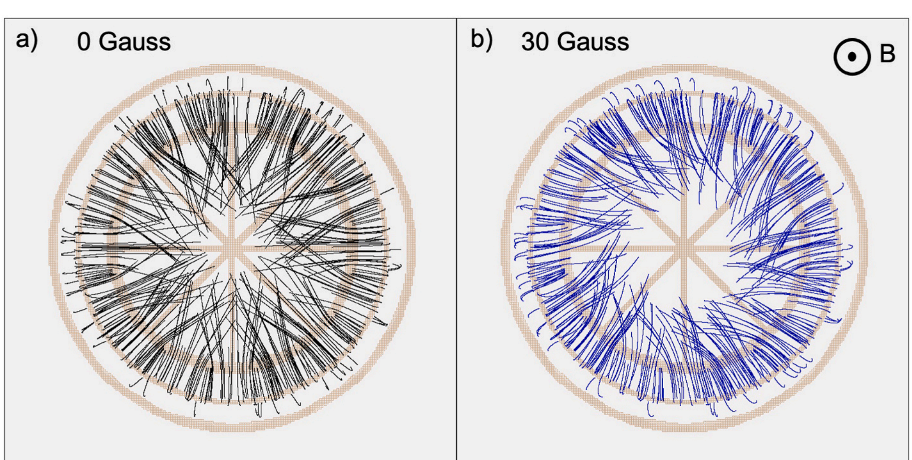


**Fig. 11.** Interrupted simulation of the electron trajectories inside the extractor gauge: a) without magnetic field; b) with magnetic field of 30 Gs along the y-axis.

trajectory under magnetic fields.

## CRediT authorship contribution statement

**Ricardo A.S. Silva:** Writing – review & editing, Writing – original draft, Visualization, Methodology, Investigation, Formal analysis, Data curation, Conceptualization. **Nenad Bundaleski:** Writing – review & editing, Visualization, Validation, Supervision, Methodology, Formal analysis, Conceptualization. **Orlando M.N.D. Teodoro:** Writing – review & editing, Validation, Supervision, Project administration, Funding acquisition.

## Declaration of competing interest

The authors declare that they have no known competing financial interests or personal relationships that could have appeared to influence the work reported in this paper.

## Data availability

Data will be made available on request.

## Acknowledgements

The support of the Portuguese Foundation for Science and Technology via the grants UIDB/00068/2020 and UIDP/00068/2020 is gratefully acknowledged. One of the authors (R. Silva) would like also to express his gratitude to the Portuguese Foundation for Science and Technology for his scholarship UI/BD/150626/2020.

## References

[1] K. Jousten, Total pressure vacuum gauges, in: Wiley-VCH (Ed.), Handbook of Vacuum Technology, second ed., 2016. Weinheim.
[2] P.C. Arnold, D.G. Bills, M.D. Borenstein, S.C. Borichevsky, Stable and reproducible Bayard-Alpert ionisation gauge, J. Vac. Sci. Technol. 12 (1994) 580–586.
[3] D. Li, K. Jousten, Comparison of some metrological characteristics of hot and cold cathode ionisation gauges, Vacuum 70 (2003) 531–541, https://doi.org/10.1016/S0042-207X(02)00781-9.
[4] J.A. Fedchak, D.R. Defibaugh, Long-term stability of metal-envelope enclosed Bayard–Alpert ionization gauges, J. Vac. Sci. Technol.: Vacuum, Surfaces, and Films 30 (2012), 061601, https://doi.org/10.1116/1.4750482.
[5] R.N. Peacock, N.T. Peacock, D.S. Hauschulz, Comparison of hot cathode and cold cathode ionization gauges, J. Vac. Sci. Technol.: Vacuum, Surfaces, and Films 9 (1991) 1977–1985, https://doi.org/10.1116/1.577439.
[6] B.R.F. Kendall, Ionization gauge errors at low pressures, J. Vac. Sci. Technol.: Vacuum, Surfaces, and Films 17 (1999) 2041, https://doi.org/10.1116/1.581912. –2049.
[7] K. Jousten, F. Boineau, N. Bundaleski, C. Illgen, J. Setina, O.M.N.D. Teodoro, M. Vicar, M. Wüest, A review on hot cathode ionisation gauges with focus on a suitable design for measurement accuracy and stability, Vacuum 179 (2020), https://doi.org/10.1016/j.vacuum.2020.109545.
[8] H. Yoshida, K. Arai, Quantitative measurements of various gases in high and ultrahigh vacuum, J. Vac. Sci. Technol.: Vacuum, Surfaces, and Films 36 (2018), 031604, https://doi.org/10.1116/1.5018210.
[9] I. Figueiredo, N. Bundaleski, O.M.N.D. Teodoro, K. Jousten, C. Illgen, Influence of ion induced secondary electron emission on the stability of ionisation vacuum gauges, Vacuum 184 (2021), https://doi.org/10.1016/j.vacuum.2020.109907.
[10] F. Watanabe, New x-ray limit measurements for extractor gauges, J. Vac. Sci. Technol.: Vacuum, Surfaces, and Films 9 (1991) 2744–2746, https://doi.org/10.1116/1.577192.
[11] P.A. Redhead, New hot-filament ionization gauge with low residual current, J. Vac. Sci. Technol. 3 (1966) 173–180, https://doi.org/10.1116/1.1492470.
[12] L.G. Pittaway, The application of ion storage in electron space-charge fields to the design of a U.H.V. gauge and mass-spectrometer ion source, Philips Res. Rep. 29 (1974) 261–302.
[13] B. Jenninger, J. Anderson, M. Bernien, N. Bundaleski, H. Dimitrova, M. Granovskij, C. Illgen, J. Setina, K. Jousten, P. Kucharski, C. Reinhardt, F. Scuderi, R.A.S. Silva, A. Stöltzel, O.M.N.D. Teodoro, B. Trzpil-Jurgielewicz, M. Wüest, Development of a design for an ionisation vacuum gauge suitable as a reference standard, Vacuum 183 (2021), https://doi.org/10.1016/j.vacuum.2020.109884.
[14] K. Jousten, M. Bernien, F. Boineau, N. Bundaleski, C. Illgen, B. Jenninger, G. Jönsson, J. Šetina, O.M.N.D. Teodoro, M. Vičar, Electrons on a straight path: a novel ionisation vacuum gauge suitable as reference standard, Vacuum 189 (2021), https://doi.org/10.1016/j.vacuum.2021.110239.
[15] W.L. Pickles, A.L. Hunt, Calibration and characterization of Bayard–Alpert gauges operating in high magnetic fields, J. Vac. Sci. Technol.: Vacuum, Surfaces, and Films 4 (1986) 1732–1735, https://doi.org/10.1116/1.573967.
[16] J. Miertusova, S. Trieste, Reliability and Accuracy of Total and Partial Pressure Measurements in the UHV Pressure Range under Real Experimental Conditions, 1998.
[17] G. Haas, H.-S. Bosch, In Vessel Pressure Measurement in Nuclear Fusion Experiments with ASDEX Gauges, 1998.
[18] H.C. Hseuh, The effect of magnetic field on the performance of Bayard-Alpert gauges, J. Vac. Sci. Technol. 20 (1982) 237–240, https://doi.org/10.1116/1.571364.
[19] R. Silva, N. Bundaleski, A.L. Fonseca, O.M.N.D. Teodoro, 3D-Simulation of a Bayard Alpert ionisation gauge using SIMION program, Vacuum 164 (2019) 300–307, https://doi.org/10.1016/j.vacuum.2019.03.039.
[20] P. Juda, B. Jenninger, P. Chiggiato, T. Richard, 3D-simulation of ionisation gauges and comparison with measurements, Vacuum 138 (2017) 173–177, https://doi.org/10.1016/j.vacuum.2016.12.014.
[21] N. Bundaleski, C.F. Adame, M. Bernien, C. Illgen, B. Jenninger, K. Jousten, F. Scuderi, R.A.S. Silva, A. Stöltzel, J. Šetina, O.M.N.D. Teodoro, T. Verbovšek, M. Vičar, M. Wüest, Novel ionisation vacuum gauge suitable as a reference standard: influence of primary electron trajectories on the operation, Vacuum 201 (2022), https://doi.org/10.1016/j.vacuum.2022.111041.
[22] R.A.S. Silva, N. Bundaleski, A. Fonseca, O.M.N.D. Teodoro, Simulation of an extractor ionisation gauge, in: 15th European Vacuum Conference (EVC-15) 17th-22th - Book of Abstracts, 2018, p. 8.
[23] NIST, Electron-impact cross sections for ionization and excitation, n.d., (accessed March 16, 2022), https://physics.nist.gov/PhysRefData/Ionization/molTable.html.
[24] L. Zhong, B. Wu, S. Zheng, Q. Gu, A database of electron-impact ionization cross sections of molecules composed of H, C, N, O, and F, Phys. Plasmas 28 (2021), https://doi.org/10.1063/5.0054342, 1ENG.